THE ASTROPHYSICAL JOURNAL, 428:L69–L72, 1994 June 20

DETECTION OF ABSORPTION BY H_2 IN MOLECULAR CLOUDS: A DIRECT MEASUREMENT OF THE H_2:CO RATIO

J. H. LACY,[1,2] R. KNACKE,[2,3] T. R. GEBALLE[2,4] AND A. T. TOKUNAGA[2,5]
Received 1994 February 11; accepted 1994 March 31

ABSTRACT

Vibrational absorption by H_2 and CO has been searched for toward infrared sources embedded in molecular clouds. H_2 was detected toward NGC 2024 IRS 2 and possibly toward NGC 2264 (GL 989). CO was detected toward both sources. The results are consistent with the H_2 ortho:para ratio being equilibrated at the cloud temperature. Toward NGC 2024, $H_2:CO = 3700^{+3100}_{-2600}$ ($2\ \sigma$ limits), and toward NGC 2264, $H_2:CO < 6000$. Approximately one-third of all carbon is in gas-phase CO.

Subject headings: infrared ISM: lines and bands — ISM: abundances — ISM: molecules

1. INTRODUCTION

Molecular hydrogen is undoubtedly the most abundant molecule in the interstellar medium. Nevertheless, its abundance has been directly measured only in diffuse clouds, which can be probed by ultraviolet absorption lines. The reason for this is well known; the absence of dipole rotational or vibrational transitions, coupled with the weakness of the quadrupole transitions, makes the opacities of H_2 lines very small, even through dense molecular clouds. In addition, the small moment of inertia of H_2 results in widely spaced rotational levels, which can be excited to emit only under unusual conditions. Because of the difficulty of observing H_2, CO has generally been used as a stand-in, and molecular abundances are typically quoted relative to CO or an assumed H_2 abundance $\sim 10^4$ times that of CO.

Although the bulk of the H_2 in molecular clouds cannot be observed in emission, it is possible to observe it in absorption against bright embedded infrared sources. Both rotational and vibrational absorption lines of H_2 may be detectable, with the vibrational lines being more favorable, due to their greater strengths. CO can also be observed in absorption, through its $v = 0$–1 and $v = 0$–2 vibrational bands. The $v = 0$–2 band is preferred for comparison with H_2 for two reasons: its wavelength proximity to the low-J H_2 lines avoids problems with observations at different wavelengths probing different depths into infrared sources, and its relatively small bandstrength alleviates uncertainties in a curve-of-growth analysis. Black & Willner (1984) and Black et al. (1990) attempted to observe H_2 $v = 0$–1 and CO $v = 0$–2 absorption toward NGC 2024 and NGC 2264. They detected CO and set limits on H_2, requiring $H_2:CO < 1.2 \times 10^4$ toward NGC 2024.

We have repeated the observations of Black & Willner and Black et al., and detected H_2 absorption toward NGC 2024 and possibly toward NGC 2264. We use these observations to make a direct determination of H_2:CO toward these sources.

2. OBSERVATIONS

Most of the observations presented here were made with CSHELL, the facility echelle spectrograph at the IRTF (Tokunaga et al. 1990), with W33 observed with CGS4 at UKIRT. CSHELL was used with its 256 × 256 HgCdTe detector array, a dispersion of $\Delta\lambda/\lambda \approx 1.2 \times 10^{-5}$ pixel^{-1}, and a slit image scale on the detector of 0".28 pixel^{-1}. The slit width was 0".5, giving a spectral resolving power of $\sim$40,000. Observations were made at the wavelengths of two H_2 lines, $S(0)$ (4497.84 cm^{-1}) and $S(1)$ (4712.91 cm^{-1}), and 15 CO lines $R(0)$–$R(8)$ (4263–4292 cm^{-1}) and $P(1)$–$P(6)$ (4235–4257 cm^{-1}).

Observations were attempted of seven sources: NGC 2024 IRS 2, NGC 2264 (GL 989), Elias 16, Mon R2, W33A, S140 (GL 2884), and VI Cygni No. 12. Of these sources, only NGC 2024 and NGC 2264 provided useful results for this project; Elias 16 showed a complicated photospheric spectrum, preventing any study of interstellar absorption, VI Cygni No. 12 showed no interstellar lines, and Mon R2, W33A, and S140 showed H_2 emission.

Comparison stars were chosen to be free of interfering spectral features, while being as close as possible to the embedded sources and at least as bright. There are no high spectral resolution surveys of stars in the K band, but visible wavelength spectra show atomic and molecular lines to be present in stars later than A0. Earlier type stars show only hydrogen and helium lines. High ($n' > 20$) Pfund-series lines fall in the region of the CO 0–2 band but are very broad and are not apparent in any of the comparison star spectra. We chose ζ Ori (B0 I, $K \approx 2$) for a comparison star for NGC 2024, and ζ Ori and γ Gem (A1, IV, $K \approx 2$) for comparison stars for NGC 2264. 15 Mon (O7 V, $K \approx 5$) and η Tau (B7 III, $K \approx 3$) also were observed. Comparison of these stars showed two absorption lines in the A1 star γ Gem near the H_2 $S(1)$ line, but not at the frequency of $S(1)$ in NGC 2264. Otherwise, no features were seen in the comparison star spectra.

The observations were made on the nights of 1993 January 24–26, all of which were clear, and October 31–November 2, most of which were cloudy or foggy. Of the results presented here, only the CO P-branch spectra and a confirming $S(0)$ spectrum were obtained on the latter run. Approximately 1 hr of on-source observation time was spent on each of the H_2 settings on each of the embedded sources. About half as much time was spent on each of the CO settings and on the comparison stars.

[1] Department of Astronomy, University of Texas, Austin, TX 78712.
[2] Visiting Astronomer at the Infrared Telescope Facility, which is operated by the University of Hawaii under contract with the National Aeronautics and Space Administration.
[3] Division of Science, Pennsylvania State University, Erie, PA 16563.
[4] Joint Astronomy Centre, Hilo, HI 96720.
[5] Institute for Astronomy, University of Hawaii, Honolulu, HI 96822.

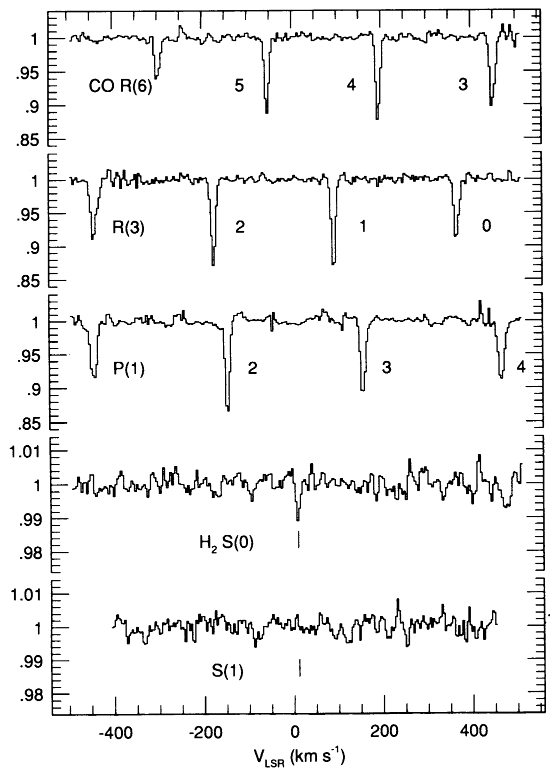

FIG. 1.—Fully processed (including fringe removal) spectra of CO $R(6, 5, 4, 3)$, $R(3, 2, 1, 0)$, $P(1, 2, 3, 4)$, and H_2 $S(0)$ and $S(1)$ toward NGC 2024 IRS 2. The horizontal scale is v_{LSR} for the H_2 lines and is arbitrary for the CO lines. The expected Doppler shift ($v_{LSR} = 10$ km s^{-1}) is marked on the H_2 spectra. Note the differing vertical scales and offsets.

The data were reduced with Snoopy (Achtermann 1992), a program written for reduction of infrared spectroscopic data. Standard procedures were used for flat-fielding, optimal weighting, and division by comparison stars. In addition, the final spectra were divided by a slowly varying function to remove interference fringes. Spectra of NGC 2024 are shown in Figure 1.

3. INTERPRETATION

Since all lines were unresolved, the information in the spectra is contained in the equivalent widths. In the case of CO, the presence of unresolved interfering telluric lines required a correction to the measured equivalent widths in addition to the division by comparison stars. To determine this correction, we modeled the telluric transmission, using the program Atmo (Grossman 1989), adjusting the water vapor until the model, convolved with the CSHELL resolution function, matched our observations of comparison stars. We then multiplied the measured equivalent widths by the ratio of calculated transmission at the wavelength of the observed CO lines to the convolved transmission. This procedure should correct for the actual telluric transmission in the case of very narrow interstellar lines, as we conclude the lines in NGC 2024 and NGC 2264 are.

If a line is optically thin, the column density in the lower state of the transition may be calculated straightforwardly from the equivalent width:

$$N_J(\mathrm{cm}^{-2}) = w_\nu(\mathrm{cm}^{-1})/S_{v,J\to v',J'} ,$$

where S is the line strength factor. For CO,

$$S_{v,J\to v',J'} = \frac{8\pi^3}{3hc}\,\nu\,\frac{\max(J, J')}{2J+1}\,|\mu_{v\to v'}|^2(\mathrm{cm}^{-1}/\mathrm{cm}^{-2}) ,$$

where ν is in cm^{-1}, and $\mu_{0\to 2} = 6.66 \times 10^{-21}$ esu cm (with a weak dependence on J; Goorvitch & Chackerian 1994). For H_2, $S_{S(0)} = 8.2 \times 10^{-26}$ cm^{-1}/cm^{-2}, and $S_{S(1)} = 4.8 \times 10^{-26}$ cm^{-1}/cm^{-2} (Turner, Kirby-Docken, & Dalgarno 1977). For optically thick lines, a saturation correction, or curve-of-growth analysis, is required. We assumed the lines to be Gaussian, and used numerical integration to determine the curve of growth.

The $S(0)$ line of H_2 was detected in absorption toward NGC 2024 IRS 2 with an equivalent width of $(2.4 \pm 0.5) \times 10^{-3}$ cm^{-1}. It was observed on three nights, with consistent results, including the expected Doppler shift change between January and November. The line was centered at $v_{LSR} = 9.5 \pm 2$ km s^{-1}, in agreement with the CO lines. A possible $S(0)$ absorption of $(0.7 \pm 0.6) \times 10^{-3}$ cm^{-1} was seen toward NGC 2264 (GL 989). The $S(1)$ line was not detected toward either source. The H_2 lines must be optically thin; the $S(0)$ equivalent width toward NGC 2024 corresponds to 0.16 km s^{-1}, whereas the H_2 thermal linewidth at the temperature of the CO is 1.0 km s^{-1} (FWHM), requiring a line-center optical depth $\lesssim 0.16$. Derived column densities are given in Table 1.

The measured CO equivalent widths are given in columns (2) and (3) of Table 2. The quoted errors are based on the noise between the lines and our estimates of the uncertainties in the correction for atmospheric absorption, with lines measured on only one night or during poor weather (in November) given higher errors. Column densities, derived assuming the lines to be optically thin, are given in columns (4) and (5), and in Figure 2.

In the case of NGC 2024, the column densities derived from the P- and R-branch lines disagree systematically, in the sense expected if the lines are saturated. We fitted the observations with equivalent widths calculated for a thermal distribution of rotational-state populations and a Gaussian-line curve of growth. A mixture of gas at two temperatures was tried but did not improve the fit. The best-fitting linewidth (e^{-1} half-width), column density, and temperature, and the allowed 2 σ ranges (over which $\chi^2 < \chi^2_{\min} + 4$) are $b = 6.9(5.1\text{–}8.6) \times 10^{-3}$ cm^{-1}, $N_{CO} = 9.1(6.1\text{–}30) \times 10^{18}$ cm^{-2}, and $T = 45(35\text{–}54)$ K. The best-fitting distribution of column densities is given in column (6) of Table 2.

The data for NGC 2264 were fitted in the same way as for NGC 2024. In this case the P : R equivalent width ratios do not require saturation, but again the best fit to the shape of the $w_\nu(J)$ distribution was obtained with a single temperature, with

TABLE 1

H_2 EQUIVALENT WIDTHS AND COLUMN DENSITIES

	NGC 2024		NGC 2264	
J	w_ν(cm^{-1})	N(10^{22} cm^{-2})	w_ν(cm^{-1})	N(10^{22} cm^{-2})
0	0.0024(5)[a]	2.9(6)	0.0007(6)	0.9(7)
1	0.0000(5)	0.0(10)	0.0000(8)	0.0(17)
Total[b]		3.5(7)		1.1(8)

[a] 1 σ uncertainties in the last digits are given in parentheses.
[b] Total H_2 column densities assuming a thermal population distribution at the CO temperature.

TABLE 2

CO Equivalent Widths and Column Densities

J (1)	w_ν[a] (cm^{-1}) P (2)	R (3)	N_J(thin)[b] (10^{18} cm^{-2}) P (4)	R (5)	N_J(fit)[c] (10^{18} cm^{-2}) (6)
NGC 2024					
0.....	...	0.015(2)	...	0.19	0.55
1.....	0.018(2)	0.021(1)	0.69	0.39	1.45
2.....	0.022(2)	0.024(2)	0.71	0.49	1.90
3.....	0.018(2)	0.020(1)	0.55	0.42	1.86
4.....	0.018(4)	0.020(2)	0.54	0.43	1.47
5.....	0.017(4)	0.018(1)	0.50	0.39	0.99
6.....	0.009(2)	0.014(2)	0.27	0.30	0.56
7.....	...	0.011(2)	...	0.24	0.28
8.....	...	0.005(2)	...	0.11	0.12
Sum			3.38		9.07
NGC 2264					
0.....	...	0.025(1)	...	0.31	0.43
1.....	0.019(3)	0.043(2)	0.73	0.80	1.07
2.....	0.020(3)	0.036(2)	0.65	0.73	1.24
3.....	0.024(3)	0.029(1)	0.74	0.61	1.00
4.....	...	0.023(1)	...	0.50	0.62
5.....	...	0.015(1)	...	0.33	0.31
6.....	...	0.003(1)	...	0.07	0.12
Sum			3.50		4.70

[a] Measured equivalent widths, with 1 σ uncertainties in the last digits, based on the estimated uncertainty in the correction for telluric absorption, given in parentheses.

[b] Column densities derived assuming the lines to be optically thin. Sum includes only observed states.

[c] Column densities for the best-fitting thermal population distribution, assuming a Gaussian-line curve-of-growth. Sum includes all rotational states.

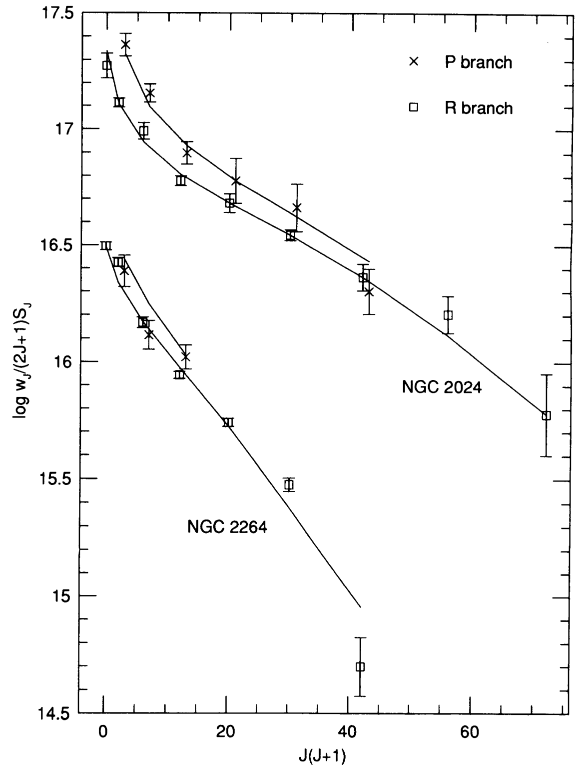

Fig. 2.—Values of log $[N_J(\text{thin}) = w_J/(2J+1)S_J]$ vs. $J(J+1)$ for NGC 2024 IRS 2 and NGS 2264 (GL 989). Results from R-branch lines are shown as squares; results from P-branch lines are shown as crosses (and are offset to the right for clarity). Results for NGC 2264 are offset downward by 1.0. If unsaturated and at a single temperature, the points would fall along a straight line. The curves through the data are calculations assuming a Gaussian-line curve of growth. For NGC 2024, $b = 6.9 \times 10^{-3}$ cm^{-1}, $N = 9.1 \times 10^{18}$ cm^{-2}, and $T = 45$ K. For NGC 2264, $b = 2.0 \times 10^{-2}$ cm^{-1}, $N = 4.7 \times 10^{18}$ cm^{-2}, and $T = 30$ K.

saturation causing the curvature of the distribution. For NGC 2264, $b = 2.0(1.5\text{–}2.6) \times 10^{-2}$ cm^{-1}, $N_{CO} = 4.7(4.0\text{–}5.8) \times 10^{18}$ cm^{-2}, and $T = 30\,(28\text{–}32)$ K. Black et al. measured the CO linewidths toward NGC 2264 to be $b = 2.5 \times 10^{-2}$ cm^{-1}, in agreement with our curve-of-growth analysis. Toward both NGC 2024 and NGC 2264, our CO results are in good agreement with those of Black & Willner and Black et al.

Several systematic errors may affect our results. For H_2, our main concern is with possible filling-in of absorption with emission. Extended or broad-lined gas would be easily recognized, and was not seen. Probably the worst case would be if narrow $S(1)$ emission (like that toward Mon R2) just canceled the absorption. However, even in this case the effect on the $S(0)$ line would be small. In emission, $S(0)$ is typically 3 times weaker than $S(1)$, whereas in absorption at the temperatures we observe, it should be $\sim$10 times stronger. Consequently, the ratio of emission to absorption for $S(0)$ would be $\sim$1/30 even in the case of equal emission and absorption for $S(1)$. For CO, the main uncertainty is in the assumption of a Gaussian line. A line with stronger wings than a Gaussian would require a greater line-center optical depth to reproduce the observed $P:R$ equivalent width ratios, and so a greater CO column density. Since our CO column densities are surprisingly large (see below), this seems unlikely. To fit our data on NGC 2024 with smaller optical depths would require a line with weaker wings than a Gaussian, but even in the extreme case of a rectangular line, our preferred value of N_{CO} would only drop to 7.5×10^{18} cm^{-2}.

4. DISCUSSION

At temperatures below 100 K, essentially all H_2 is in the $J = 0$ and $J = 1$ states. Consequently, the H_2 ortho:para ratio is given by the ratio of the populations of these two states. Our limit on the $J = 1 : J = 0$ ratio toward NGC 2024, <0.8 (2 σ), is significantly less than the expected ortho:para ratio of 3 when H_2 first forms, and is consistent with the value of 0.2 expected if it is thermalized at the temperature of the CO. Two processes are thought to be most important in modifying the ortho:para ratio in cold clouds: proton exchange reactions with H^+ and H_3^+, equilibrating ortho:para at the gas temperature, and interaction with magnetic impurities in grains, equilibrating ortho:para at the grain temperature (Burton, Hollenbach, & Tielens 1992). These processes are expected to equilibrate ortho:para in a time short compared to the lifetime of a molecular cloud. Our observations are consistent with this prediction.

For the purpose of determining the most probable value of N_{H_2} (H_2:CO), we assume that $J = 1 : J = 0$ is thermalized at the CO temperature; estimated grain temperatures are about equal to the gas temperatures (Thronson et al. 1984; Sargent et al. 1984). With this assumption, and using only our $S(0)$ measurement, we obtain $N_{H_2} = (3.5 \pm 1.4) \times 10^{22}$ cm^{-2} toward NGC 2024, and $<2.4 \times 10^{22}$ cm^{-2} toward NGC 2264 (2 σ uncertainties).

To determine the H_2:CO ratio, we fitted the H_2 and CO equivalent widths simultaneously. Toward NGC 2024 IRS 2, the best-fitting value of H_2: CO is 3900, with an allowed (2 σ) range of 1300–6800. The value of χ^2 for the fit is 10.6 for 12 degrees of freedom, indicating that the model fits the data well and the noise was estimated reasonably . Toward NGC 2264, the best-fitting value of H_2: CO is 1800, but N_{H_2} (and so H_2: CO) differs from 0 only at the 1 σ level. The upper limit on H_2: CO is 5200.

There are few other determinations of H_2: CO with which we can compare our measurements. Frerking, Langer, & Wilson (1982) compare the column densities of various CO isotopes with A_v, and obtain $N_{C^{18}O}/A_v = 1.7 \times 10^{14}$ cm^{-2} in cloud interiors ($A_v > 4$). This corresponds to $N_{CO}/A_v = 8.3 \times 10^{16}$ cm^{-2}, and H_2: CO = 12,000 if the low-A_v ratio of $N_H/A_v = 1.9 \times 10^{21}$ cm^{-2} (Bohlin, Savage, & Drake 1978) is assumed. Watson et al. (1985) made a direct measurement of H_2: CO = 8000 in the shocked gas in Orion, but it is unlikely that the abundances of H_2 and CO there are typical of molecular clouds. Wilson et al. (1986) observed warm gas in the same region, and obtained H_2: CO = 20,000. Most other papers on the subject (see van Dishoeck & Black 1987), discuss N_{H_2}/I_{CO}, not N_{H_2}/N_{CO}, and bypass the determination of I_{CO}/N_{CO}.

It is also of interest to compare N_{H_2} and N_{CO} to estimates of A_v toward our sources. The extinction to NGC 2264 (GL 989) is highly uncertain, with values in the literature ranging from $A_v = 5$ to $A_v > 35$. McGregor, Persson, & Cohen (1984) point out the complexity of the source, which in the near-infrared has diffuse extended emission and a pointlike condensation that is not coincident with the mid-infrared source.

Jiang, Perrier, & Lena (1984) measured $A_v = 21.5 \pm 5$ to NGC 2024 IRS 2, based on modeling to speckle interferometry and photometry. About half of the extinction may be due to circumstellar material (which may or may not contain H_2 and CO), as Maihara, Mizutani, & Suto (1990) used Brγ/Brα to derive $A_v \approx 11$ for the extended ionized gas surrounding the source. Assuming $A_v = 21.5$, we obtain $N_{H_2}/A_v \approx 1.7 \times 10^{21}$ cm^{-2} and $N_{CO}/A_v \approx 4.3 \times 10^{17}$ cm^{-2}, with uncertainties of factors $\sim$2. Our N_H/A_v is about 1.8 times that measured by Bohlin et al., whereas our N_{CO}/A_v is about 5 times that measured by Frerking et al. These results suggest that the gas-to-dust ratio toward NGC 2024 is nearly normal, and that it is the CO abundance that is surprising.

The N_{CO}/A_v ratios through the NGC 2024 and 2264 molecular clouds can also be estimated from longer wavelength observations. Toward NGC 2024 FIR 5, Graf et al. (1993) derived $N_{CO} = 2 \times 10^{19}$ cm^{-2} from CO emission, and Thronson et al. (1984) derived $A_v \approx 100$ from 60 μm dust emission, giving $N_{CO}/A_v \approx 2 \times 10^{17}$. A similar N_{CO}/A_v ratio, 2.2×10^{17}, through NGC 2264 is obtained from the results of Sargent et al. (1984) and Krügel et al. (1987). Both numbers are less than our determination, but probably not significantly so given the large uncertainty in the interpretation of the continuum observations.

Finally, our H_2: CO ratio may be compared to the solar H: C ratio of 2500 (Grevesse et al. 1991). Assuming all H to be in H_2, we conclude that about one-third of all carbon is in gas-phase CO. Although uncertain by a factor $\sim$2, this is a considerably larger fraction of carbon in CO than previously estimated. The column density of solid CO toward NGC 2024 is small (Tielens et al. 1991), but gas-phase C and C^+ together may be comparable to CO in abundance (Jaffe et al. 1994), suggesting that graphite and carbonate grains may contain only about one-third of all carbon.

We are grateful to D. Griep and W. Golisch for assistance with the observations, T. Greene for assistance in the use of CSHELL, and J. Achtermann for modifying Snoopy for reduction of CSHELL data. We also than the referee, S. P. Willner, for pointing out a significant error in the original *Letter*, and E. van Dishoeck and G. Mitchell for helpful discussions. This work was supported by grants from the NSF and USAF.

REFERENCES

Achtermann, J. M. 1992, in Astronomical Data Analysis and Software, ed. D. M. Worrall, C. Biemesderfer, & J. Barnes (ASP Conf. Ser., 25), 451
Black, J. H., van Dishoeck, E. F., Willner, S. P., & Woods, R. C. 1990, ApJ, 358, 459
Black, J. H., & Willner, S. P. 1984, ApJ, 279, 673
Bohlin, R. C., Savage, B. D., & Drake, J. F. 1978, ApJ, 224, 132
Burton, M. G., Hollenbach, D. J., & Tielens, A. G. G. M. 1992, ApJ, 399, 563
Frerking, M. A., Langer, W. D., & Wilson, R. W. 1982, ApJ, 262, 590
Goorvitch, D., & Chakerian, C. 1994, ApS, 91, 483
Graf, U. U., Eckart, A., Genzel, R., Harris, A. I., Poglitsch, A., Russell, A. P. G., & Stutzki, J. 1993, ApJ, 405, 249
Grevesse, N., Lambert, D. L., Sauval, A. J., van Dishoeck, E. F., Farmer, C. B., & Norton, R. H. 1991, A&A, 242, 488
Grossman, E. 1989, private communication
Jaffe, D. T., Zhou, S., Howe, J. E., Herrmann, F., Madden, S. C., Poglitsch, A., van der Werf, P. P., & Stacey, G. J. 1994, preprint
Jiang, D. R., Perrier, C., & Lena, P. 1984, A&A, 135, 249
Krügel, E., Güsten, R., Schulz, A., & Thum, C. 1987, A&A, 185, 283
Maihara, T., Mizutani, K., & Suto, H. 1990, ApJ, 354, 549
McGregor, P. J., Persson, S. E., & Cohen, J. G. 1984, ApJ, 286, 609
Sargent, A. I., Van Duinen, R. J., Nordh, H. L., Fridlund, C. V. M., Aalders, J. W. G., & Beitema, D. 1984, A&A, 135, 377
Thronson, H. A., Lada, C. J., Schwartz, P. R., Smith, H. A., Smith, J., Glaccum, W., Harper, D. A., & Loewenstein, R. F. 1984, ApJ, 280, 154
Tielens, A. G. G. M., Tokunaga, A. T., Geballe, T. R., & Baas, F. 1991, ApJ, 381, 181
Tokunaga, A. T., Toomey, D. W., Carr, J., Hall, D. N. B., & Epps, H. W. 1990, Proc. SPIE, 1235, 131
Turner, J., Kirby-Docken, K., & Dalgarno, A. 1977, ApJS, 35, 281
van Dishoeck, E. F., & Black, J. H. 1987, in Physical Processes in Interstellar Clouds, ed. G. E. Morfill & M. Scholer (Dordrecht: Reidel), 241
Watson, D. M., Genzel, R., Townes, C. H., & Storey, J. W. V. 1985, ApJ, 298, 316
Wilson, T. L., Serabyn, E., Henkel, C., & Walmsley, C. M. 1986, A&A, 158, L1